AN IMPROVED STOCHASTIC MODEL FOR MULTI-PASS RADAR INTERFEROMETRY

R.F. Hanssen
Delft Institute for Earth-Oriented Space Research, Delft University of Technology,
P.O. Box 5030, 2600 GA Delft, The Netherlands
hanssen@geo.tudelft.nl

KEYWORDS: Radar, Interferometry, Deformation monitoring, Digital Elevation Models

ABSTRACT

Radar interferometry has evolved significantly during the late 80's and in the 90's. The applications of the technique have broadened, starting from topographic mapping using single-pass, dual antenna, airborne configurations, to deformation mapping and atmospheric water vapor mapping using multi-pass spaceborne configurations. The full geodetic validation of the technique, however, requires proper modeling of the dispersion of the data, i.e., the full variance covariance matrix. Although single-look and multi-look phase statistics have been discussed by many authors, parameter estimation using a Gauss-Markov model also requires the stochastic modeling of the covariance between resolution cells.

In this paper, we will present a first stochastic model which takes into account how spatial (de)correlation can be accounted for. Spatial decorrelation caused by propagation delay heterogeneities is especially important when analyzing deformation processes over long time intervals. In these situations, the interpretation of the interferometric phase is often hampered by temporal decorrelation, which produces isolated relatively coherent patches surrounded by areas where coherence is lost entirely.

Spatial correlation functions are derived using interferogram sets in which the propagation delay variability could be modeled. Although this variability seems to be non-stationary at these scales, it appears to have scaling and power-law properties. Using spatial structure functions, these properties are translated to the variance-covariance matrix. Special emphasis is on the factor which needs to be applied to scale the variances. Localized coherent areas might often be sufficient to provide a first estimate for this factor, even in severely decorrelated interferograms.

This procedure results in an improved description of radar interferometry, described as a parameter estimation problem. It is shown how such considerations might lead to the assessment whether radar interferometry is a suitable tool for, e.g., specific deformation problems. The method can be applied for different geophysical deformation problems, caused by ground water extraction, gas exploration and volcanic deformation.

1 INTRODUCTION

For geodetic analysis of measurements, the most important issue is the construction of a mathematical model which relates the observations to the unknown parameters. Using the Delft method, we divide such a mathematical model in two parts: the functional model and the stochastic model. Written as a standard Gauss-Markov model, the (linearized) functional model is written as:

$$\underline{y} = Ax + \underline{\varepsilon}; \tag{1}$$

where $\underline{y}$ and $\underline{\varepsilon}$ are the stochastic observations and errors, respectively, A is the design matrix which relates the observations to the parameters x, which are assumed to be deterministic. If we expect that the errors $\underline{\varepsilon}$ have a zero-mean distribution, the expectation $E\{.\}$ of the observations is:

$$E\{\underline{y}\} = Ax. \tag{2}$$

The stochastic model describes the dispersion, or second moment, of the observations:

$$D\{\underline{y}\} = Q_y; \tag{3}$$

where Q_y is the full variance-covariance matrix. If the observations are not correlated, Q_y will be a diagonal matrix. Correlations between observations result in a full-matrix. For n observations, Q_y will be an $n \times n$ matrix. For m unknown parameters, we find the redundancy $r = n - m$. The significance of the Gauss-Markov model is the sheer amount of adjustment and hypothesis testing routines which are readily available for problems formulated in this form. In this discussion, we won't discuss this in more detail. Instead, our goal is to find the best way to write our problem in the form of equation (2) and (3).

1.1 Problem formulation for radar interferometry

Until to date, the functional model for radar interferometry described the relation between the observations $\underline{y}$: the (unwrapped) phase of a resolution cell, and the parameters x. In the repeat-pass configuration, phase variability is considered to be caused by topographic height x_h or deformation x_d. The variance of the observations σ_y^2 is derived from the local coherence in the interferogram.

Several problems appear in this formulation of the functional and stochastic model. First, every observed phase $\underline{y}_i$ in resolution cell i is connected with two unknown parameters: x_h and x_d. This gives n observations and $2n$ parameters, and therefore the problem is underdetermined. Second, it has been shown by several authors that atmospheric delay variation influences the observed phase considerably, and can cause up to 5 phase cycles errors. Inclusion of the

atmospheric delay x_a in the functional model raises the amount of unknown parameters to $3n$. A third problem is concerned with phase unwrapping. All currently used algorithms use heuristic assumptions of a maximally allowable phase gradient. Although this assumption might hold for a large number of situations, it is doomed to fail in, e.g., foreshortening regions and regions with strong deformation. In order to write the functional model in more robust terms, it is necessary to include the unknown integer ambiguity of the phase k, with $\phi = \phi_{fr} + k2\pi$, as an unknown parameter. In this expression, ϕ_{fr} is the so-called *fractional* or observed phase, and $k2\pi$ is the fixed integer phase. This approach raises the amount of unknown parameters to $4n$, and the problem is even more underdetermined.

The solution to the first problem is rather pragmatic. For deformation measurements, it is often assumed that the topographic height is known in advance. For topographic height measurements, it is assumed that no deformation occurred between the two acquisitions. A more advanced solution to the redundancy problem is the use of several interferograms: l interferograms increase the number of observations to ln, whereas the topgraphic height x_h does not change.

The second problem, atmospheric signal, is more difficult to eliminate, as every new interferogram introduces a new set of atmospheric parameters x_a. Therefore, an increase in the number of interferograms will simultaneously increase the number of parameters. As long as no useful (high-resolution, quantitative) atmospheric data are available from other sources, attempts to resolve the atmospheric parameters in the functional model will be difficult and rather ad hoc. An alternative solution is presented here, where we move the atmospheric uncertainties from the functional to the stochastic model. The following paragraphs will expand on this idea.

For completeness, we remark that we will leave the problem of the integer phase ambiguities outside the scope of this discussion. For now, we assume that phase unwrapping yields sufficiently accurate results.

1.2 Parametrization of spatial correlation

This paper will summarize ideas on the use of structure functions, power spectra, and covariance analysis. We propose to include the spatial variation of the atmospheric signal in the stochastic model. In an interferogram, the functional model relates the observations (phase values for every pixel) to the unknown parameters (e.g., the parameters of a deformation model). The stochastic model appoints a variance for every single pixel and covariances between any combination of two pixels. The determination of the variance values is well described in literature, see, e.g., Just and Bamler (1994). Covariance values, however, have rarely been discussed in the field of radar interferometry. Partially this is due to the fact that the type and magnitude of atmospheric signal has long been underestimated.

In section 2, we discuss how the power spectrum and the structure function are related. The structure function will be related to the correlation function and covariance function in section 4

2 POWER SPECTRUM AND STRUCTURE FUNCTION

2.1 Definitions

There is a specific class of signals $\varphi(x)$ with a power-law behavior, i.e., their power spectrum $P_\varphi(f)$ has the following form (Agnew 1992):

$$P_\varphi(f) = P_0(f/f_0)^\nu. \tag{4}$$

In this equation, f is some (spatial or temporal) frequency, P_0 and f_0 are normalizing constants, and ν is the *spectral index*; often $-3 < \nu < -1$. Here we show the relationship between this power-law signal $\varphi(x)$, and its structure function, which behaves as (Monin and Yaglom 1975; Agnew 1992)

$$D_\varphi(R) = C_\nu \frac{P_0}{f_0^\nu} R^{-(\nu+1)}. \tag{5}$$

This relation and the definition of the structure coefficient C_ν is derived in section 10.

The structure function $D_\varphi(R)$ of $\varphi(x)$ is defined as

$$D_\varphi(R) = < [\varphi(x+R) - \varphi(x)]^2 >, \tag{6}$$

where $< \cdot >$ denotes the ensemble average over all realizations. Hence, we can also denote (6) using the expectation E notation

$$D_\varphi(R) = E\{[\varphi(x+R) - \varphi(x)]^2\}. \tag{7}$$

We can consider the behavior of a new signal $\phi_R(x)$ defined by

$$\phi_R(x) = \varphi(x+R) - \varphi(x), \tag{8}$$

which is the variation of x over a fixed interval R. The relevance of this substitution is that while $\varphi(x)$ might be non-stationary (when $\nu \leq -1$, see section 3), $\phi_R(x)$ is often stationary. This implies that the expectation $\mathrm{E}\{\varphi(x)\}$ can differ considerably depending on the position x, whereas the expectation $\mathrm{E}\{\phi_R(x)\}$ for a fixed interval R is believed to be constant. For radar interferometry, $\varphi(x)$ would be the behavior of the signal delay depending on the position in the image x (which cannot be measured in an absolute sense in an interferogram, but can be measured, e.g., in a GPS signal), whereas $\phi_R(x)$ is the difference between two points in the interferogram (or two GPS receivers) at an interval R.

2.2 Synthetic example power spectrum vs. structure function: fractional Brownian motion

In Fig. 1 we simulated data with fractional Brownian motion characteristics (where $-3 < \nu < -1$ in eq. (4) and (5), according to Mandelbrot and Ness (1968)). Note that any spectrum with $\nu < -1$ must be non-stationary (Ishimaru 1978, p. 523). The power spectrum is plotted on a loglog scale in Fig. 1b. We defined $f_0 = 1$ km and found the corresponding value $P_0 = 210.7$ rad^2, and the exponent $\nu = -1.70 \approx -5/3$, as indicated in 1c. Using eq. (5), we can predict the structure function $D(x)$, which is plotted using a straight line in 1d. The numerical evaluation of the structure function based on the original data is overlayed as the striped-dotted line.

3 STATIONARITY CONSIDERATIONS

For a stationary function, the ensemble averages (or expectation value) of a series with length N are independent of the position x of this series. In fact, for strictly stationary functions, the whole *probability density function* is independent of the position x. The question is now whether one realization, say, an interferogram, can be considered stationary. Unless we have infinitely many sample functions available which last until infinity, it is never possible to answer this question (Newland 1993). One practical consideration is to compare the extent of the observations with the period of its lowest frequency spectral components. If the period is much larger than the period of its lowest frequency spectral components, it can be assumed that the process is approximately stationary over most of its range.

Using the spectral index of the power spectrum, we can make a first statement on stationarity. For stationary functions, the power spectrum has a spectral index $\nu > -1$. For functions with stationary increments, the spectral index $\nu > -3$ (Ishimaru 1978, p.523),(Agnew 1992).

It is important to note that stationarity is a property of the random function or process, not the data. Testing whether a specific process is stationary is often difficult, as we need several realizations of the random process.[1] In our case, for spatial tropospheric delay variation, we used a set of 26 interferograms and analyzed them. As the data are inherently relative, mean values will often be zero, but higher order moments vary considerably depending on the weather situation. Four rotationally averaged power spectra are shown in figure (8–11). From this study, see Hanssen (1998), we conclude that tropospheric delay variation, and therefore the spatial variation of refractivity, is non-stationary on scales of 100 m to 200 km.

Another consideration on stationarity is the analysis of the nature of tropospheric delay. As the troposphere is a thin layer (less than 8 km) over the whole earth, the total tropospheric delay function at time t has only one first moment, one second moment, etc. It is expected that these moments remain constant for different time evaluations.

The final consideration concerns the data adjustment using the Gauss-Markov model, see equations (2) and (3). In order to use this model, the expection $E\{\underline{\varepsilon}\} = 0$ is a necessary restriction. Therefore, whereas stationarity only requires a constant first moment, in the Gauss-Markov model the requirement that the first moment has a null-value is even more strict. On the other hand, the Gauss-Markov model does not dictate anything for second and higher order moments.

For radar interferometry, the latter considerations are favourable: an interferogram is an inherently relative measurement. It is only possible to measure phase differences between pixels. Therefore, the mean value of the total interferogram can be easily set to 0 rad. Moreover, phase ramps which could be caused by orbit errors are removed from the interferogram as well. The resulting interferogram seems sufficiently adapted for standard testing and adjustment.

4 RELATION OF STRUCTURE FUNCTION WITH CORRELATION FUNCTION

If we define F as the set of random functions, G as the set of random functions with stationary increments, introduced by Kolmogorov (1941), and K as the set of stationary random functions, we can write, see Fig. 2:

$$K \in G \in F. \tag{9}$$

Random functions with stationary increments can be considered as a generalization of stationary functions, in which conditions are somewhat relaxed. Here we assume that, although the signal is not stationary, the *variation* of the signal over a fixed interval is stationary.
For the definition of the structure function, we repeat (6):

$$D_\varphi(R) = < [\varphi(x+R) - \varphi(x)]^2 > \tag{10}$$

We can rewrite this as:

$$\begin{aligned} D_\varphi(R) &= < [\varphi^2(x+R) + \varphi^2(x) - 2\varphi(x)\varphi(x+R)] > \\ &= < \varphi^2(x+R) > + < \varphi^2(x) > \\ &\quad -2 < \varphi(x)\varphi(x+R) > \\ &= 2[< \varphi^2(x) > - < \varphi(x)\varphi(x+R) >]. \end{aligned} \tag{11}$$

Defining the (auto)correlation function as

$$B_\varphi(R) = < \varphi(x)\varphi(x+R) >, \tag{12}$$

we can write

$$D_\varphi(R) = 2[B_\varphi(0) - B_\varphi(R)]. \tag{13}$$

Hence, for *stationary* signals, knowledge of the correlation function $B_\varphi(R)$ implies knowledge about the structure function $D_\varphi(R)$ as well. It doesn't necessarily work the other way: eq. (13) does not uniquely determine $B_\varphi(R)$, unless $B_\varphi(\infty) = 0$ (Monin and Yaglom 1975; Ishimaru 1978).
In short we can summarize

- for a stationary function, both the correlation function and the structure function exist, while
- for a non-stationary process with stationary increments, the structure function exists, but the correlation function does not exist.

5 INTERFEROGRAMS: ADDITION OF POWER LAWS

Here we investigate what power law relation we would expect in an interferogram: the *sum* of two atmospheric states.
An interferogram is the complex multiplication of two complex SAR images. If in each SAR image, the atmospheric delay $y(x)$ can be written as

$$y_1(x) \overset{F,power}{\longrightarrow} P_1 (\frac{f}{f_2})^\nu \tag{14}$$

then the addition theorem (Bracewell 1986) gives

$$(y_1(x) + y_2(x)) \overset{F,power}{\longrightarrow} P_1 (\frac{f}{f_1})^\nu + P_2 (\frac{f}{f_2})^\nu \tag{15}$$

If we take the normalization frequency f_0 equal in both signals we find:

$$(y_1(x) + y_2(x)) \overset{F,power}{\longrightarrow} (P_1 + P_2)(\frac{f}{f_0})^\nu \tag{16}$$

Therefore, the exponent does not change, only the P_0 value.

[1] Computing a mean on one set of (spatial) data is a *spatial* average, and not an *ensemble* average. Stationarity pertains to the invariance of the ensemble average.

Note that the *similarity theorem* is used when scaling a signal, e.g., when transforming a GPS delay time series to spatial variation using the wind speed:

$$g(a\cdot x) \xrightarrow{F} \frac{1}{|a|}\cdot S(\frac{f}{a}) \xrightarrow{power} \frac{1}{a^2}\cdot |S(\frac{f}{a})|^2 = \frac{P_0}{a^2}\cdot(\frac{f}{af_0})^{\nu} \tag{17}$$

However, this means that the same $P(f)$ values will end up at a different frequency. When viewed using double-logarithmic axes, this corresponds with a simple shift of the curve. The exponent ν won't change.

6 KOLMOGOROV SPECTRUM

In the case of isotropic turbulence in three dimensions, Kolmogorov turbulence theory predicts a specific structure function. For the Kolmogorov spectrum, the structure function $D_N(r)$ of the variation of the refractivity N is given by (Tatarski 1961, p. 75)

$$\begin{aligned} D_N(r) &= <[N(\vec{r}+\vec{r_1})-N(\vec{r_1})]^2> & (18)\\ &= C_N\cdot r^{2/3} \quad \text{for} \quad l_i \ll r \ll l_o & (19)\\ &= C_N^2\cdot l_i^{2/3}(r/l_i)^2 \quad \text{for} \quad r \ll l_i, & (20)\end{aligned}$$

where l_i and l_o are the inner and outer scales of turbulence (Ishimaru 1978; Tatarski 1961; Treuhaft and Lanyi 1987; Ruf and Beus 1997) Equation (19) was developed by Kolmogorov (1941) and Obukov (1941), and is usually referred to as the 'two-thirds law'. The exponent 2/3 expresses the rate at which the refractivity decorrelates with increasing distance.

The inner and outer scales are defined differently in various literature sources. Ruf and Beus (1997) indicated an outer scale in the order of tens of meters, whereas Treuhaft and Lanyi (1987) simply referred to scales much smaller than the effective height of the wet troposphere, which is in the order of km's. Note, however, that the equations (18–20) were defined for isotropic 3D turbulence. For horizontal scales commonly associated with, e.g., GPS and radar interferometry, the spatial distances are often larger than the effective height of the wet troposphere (1–3 km). This results in effective 2D turbulence, a property which is observed by several authors.

7 STRUCTURE FUNCTION OF THE SIGNAL DELAY

Assuming the Kolmogorov relation for 3D turbulence, within the inner and outer scales, we used

$$D_N(r) =< [N(\vec{r}+\vec{r_1})-N(\vec{r_1})]^2 >= C_N\cdot r^{2/3}, \tag{21}$$

where C_N is a measure for the 'roughness' of the spatial inhomogeneities. In Fig. 3 three examples of this equation are given for arbitrary values. In the sequel, we will assume that C has a constant value over all distances $\vec{r}$. The value of C for different realizations can be determined from the interferogram data. Furthermore, in the derivation below we will assume that $E\{N(\vec{r})\}$ or $<N(\vec{r}>$ is independent of the position $\vec{r}$ (Treuhaft and Lanyi 1987)[2]. The tropospheric delay τ at location $\vec{x}$ on the Earth's surface from a satellite at elevation angle θ and azimuth ϕ is written as

$$\tau(\vec{x}) = \frac{1}{\sin\theta}\int_0^h N(\vec{x}+\vec{R}(\theta\phi,z)dz. \tag{22}$$

Note that $\vec{x}$ is a 2D vector on the flat earth, h is the effective height of troposphere.

For two positions (pixels) with distance ρ, the expectation E for the quadratic difference of the delay between the two positions is the *structure function*:

$$D_\tau(\rho) =< [\tau(\vec{x}+\vec{\rho})-\tau(\vec{x})]^2 > . \tag{23}$$

It can be shown that the structure function of the delay $D_\tau(\rho)$, eq. (23) can be related to the structure function of the refractivity $D_N(R)$, eq. (21):

$$D_\tau(\rho) = \frac{1}{\sin^2\theta}\int\int [D_N(R_2)-D_N(R_1)]dzdz'. \tag{24}$$

The geometric configuration used in this equation is shown in Fig.4.

The following derivation shows how the structure function of the delay $D_\tau(\rho)$ can be related to the structure function of the refractivity $D_N(R)$.

7.1 Derivation

Starting from the definition of the structure function in eq. (23) we substitute eq. (22):

$$\begin{aligned} D_\tau(\rho) &= <[\frac{1}{\sin\theta}\int_0^h N(\vec{x}+\vec{\rho}+\vec{r}(\theta,\phi,z))dz - \\ &\quad \frac{1}{\sin\theta}\int_0^h N(\vec{x}+\vec{r}(\theta,\phi,z))dz]^2 > \\ &= <\frac{1}{\sin^2\theta}\int_0^h N^2(\vec{x}+\vec{\rho}+\vec{r}(\theta,\phi,z))dz \\ &\quad +\frac{1}{\sin^2\theta}\int_0^h N^2(\vec{x}+\vec{r}(\theta,\phi,z))dz \\ &\quad -\frac{2}{\sin^2\theta}\int_0^h N(\vec{x}+\vec{\rho}+\vec{r}(\theta,\phi,z))dz \\ &\quad \times\int_0^h N(\vec{x}+\vec{r}(\theta,\phi,z))dz > . \end{aligned} \tag{25}$$

As the expectation of a sum is equal to the sum of the expectations, we can exchange integration and expectation (or ensemble average):

$$\begin{aligned} D_\tau(\rho) &= \frac{1}{\sin^2\theta}[\int_0^h <N^2(\vec{x}+\vec{\rho}+\vec{r}(\theta,\phi,z))>dz \\ &\quad +\int_0^h <N^2(\vec{x}+\vec{r}(\theta,\phi,z))>dz \\ &\quad -2\iint_{0\to h} <N(\vec{x}+\vec{\rho}+\vec{r}(\theta,\phi,z_1)) \\ &\quad \times N(\vec{x}+\vec{r}(\theta,\phi,z_2))>dz_1dz_2]. \end{aligned} \tag{26}$$

By assuming that $<N^2>$ is independent of the position and writing the integral outside of the summation, we can

[2] This assumption does not hold always RH, but is (only) important for the calculation of the tropospheric covariance.

simplify eq. (26) to

$$\begin{aligned} D_\tau(\rho) &= \frac{1}{\sin^2\theta}[2\int_0^h < N^2(\vec{x}+\vec{r}(\theta,\phi,z)) > dz \\ &\quad -2\iint\limits_{0\to h} < N(\vec{x}+\vec{\rho}+\vec{r}(\theta,\phi,z_1)) \\ &\quad \times N(\vec{x}+\vec{r}(\theta,\phi,z_2)) > dz_1 dz_2] \\ &= \frac{1}{\sin^2\theta}\iint\limits_{0\to h}[2 < N^2(\vec{x}+\vec{r}(\theta,\phi,z_1)) > dz_1 \\ &\quad -2 < N(\vec{x}+\vec{\rho}+\vec{r}(\theta,\phi,z_1)) \\ &\quad \times N(\vec{x}+\vec{r}(\theta,\phi,z_2)) >]dz_1 dz_2. \end{aligned} \quad (27)$$

For stationary signals we can write the structure function of N, eq. (21), as

$$D_N(R) = 2 < N^2(\vec{r} > -2 < N(\vec{r}+\vec{R})N(\vec{r}) >, \quad (28)$$

8 TREUHAFT AND LANYI MODEL

A structure function model has been introduced by Treuhaft and Lanyi (1987):

$$\log(D_\tau(\alpha)/C^2 h^{8/3}) = \sum_{i=0}^{10} a_i (\log\alpha)^i, \quad (29)$$

where the variable α is the ratio of the horizontal distance ρ with the effective height of the wet troposphere h ($\alpha = \rho/h$). The polynomial coefficients for a delay in zenith direction are found in Table 1.

9 ANALYSIS EMPIRICALLY DERIVED STRUCTURE FUNCTIONS

We analyzed eight interferogram segments of 50 × 50 km over Groningen in the Northern part of the Netherlands, and derived the two dimensional structure functions for these segments. From these we used a rotational average to obtain a one-dimensional structure function. Figures 5 and 6 show the results for all eight interferograms. The TL model used an effective height [3] of the wet troposphere of 1000 m, and $C = 2.4e-07$ m$^{-1/3}$, cf. equation (29). This value for C was derived using the standard deviation of the zenith wet delay over a given time interval for sites at midlatitudes (California, Australia and Spain). It can be observed that these standard parameters are not directly applicable for a coastal zone area such as the Netherlands.

10 RELATIONSHIP BETWEEN POWER LAW SPECTRAL FORM AND STRUCTURE FUNCTION.

To relate the structure function $D_\varphi(R)$, also written as $< \phi_R^2 >$, to the power-law spectral form of equation (4), we can rewrite $\phi_R(x)$ in equation (8) in a more general form using the convolution notation (Bracewell 1986), see Fig. 7:

$$\phi_R(x) = \varphi(x) * [\delta(x-R) - \delta(x)]. \quad (30)$$

Now, we can write the power spectrum of $\phi_R(x)$ as

$$P_\phi(f) = |G_R(f)|^2 P_\varphi(f), \quad (31)$$

the multiplication of the power spectrum of $\varphi(x)$, $P_\varphi(f)$, and the power spectrum of $[\delta(x-R)-\delta(x)]$, denoted by $|G_R(f)|^2$, where

$$[\delta(x-R)-\delta(x)] \xrightarrow{F} G_R(f). \quad (32)$$

Using $\delta(x) \xrightarrow{F} 1$, and using the shift theorem (Bracewell 1986), we find

$$\delta(x-R) \xrightarrow{F} e^{-j\omega R}\cdot 1, \quad (33)$$

and using the linearity conditions of Fourier transforms we obtain

$$[\delta(x-R)-\delta(x)] \xrightarrow{F} e^{-j\omega R} - 1. \quad (34)$$

Using $e^{-j\omega R} = \cos\omega R - j\sin\omega R$ we can retrieve the power spectrum $|G_R(f)|^2$ by complex multiplication

$$\begin{aligned} |G_R(f)|^2 &= (\cos\omega R - 1 - j\sin\omega R)(\cos\omega R - 1 + j\sin\omega R) \\ &= 2 - 2\cos\omega R \\ &= 4\frac{1}{2}(1-\cos(2\omega\frac{1}{2}R)) \\ &= 4\sin^2(\frac{1}{2}\omega R) \\ &= 4\sin^2(\pi f R) \end{aligned} \quad (35)$$

Hence, the power spectrum of $\phi_R(x)$, see (31) is given by

$$P_\phi(f) = 4\sin^2(\pi f R) P_\varphi(f), \quad (36)$$

The variance of a random process ϕ_R is equal to the integral of its power spectrum over all frequencies, using (35):

$$< \phi_R^2 >= \int_0^\infty P_\phi(f)df = \int_0^\infty 4P_\varphi(f)\sin^2(\pi f R)df. \quad (37)$$

If we now insert the special power spectral form of (4), we can write (37) as

$$< \phi_R^2 >= \int_0^\infty 4P_0(f/f_0)^\nu \sin^2(\pi f R)df. \quad (38)$$

Substituting $u = \pi f R$ this can be written as

$$< \phi_R^2 >= \int_0^\infty 4P_0 u^\nu (\pi R)^{-\nu} f_0^{-\nu}\pi^{-1}R^{-1}\sin^2(u)du. \quad (39)$$

or, as in Agnew (1992)

$$< \phi_x^2 >= \frac{4P_0}{f_0^\nu}\frac{R^{-(\nu+1)}}{\pi^{\nu+1}}\int_0^\infty u^\nu \sin^2 u du. \quad (40)$$

We use the following definite integral (Gradshteyn, Ryzhik, and Jeffrey 1994, eq. 3.823)

$$\int_0^\infty x^{\mu-1}\sin^2 ax dx = -\frac{\Gamma(\mu)\cos\frac{\mu\pi}{2}}{2^{\mu+1}a^\mu} \quad [a>0, -2 < \mathrm{Re}\{\mu\} < 0] \quad (41)$$

with $\nu = \mu - 1$ and $a = 1$, yielding

$$\begin{aligned} < \phi_R^2 > &= \frac{4P_0}{f_0^\nu}\frac{R^{-(\nu+1)}}{\pi^{\nu+1}}\frac{\Gamma(\nu+1)\cos(\nu\pi/2+\pi/2)}{2^{\nu+2}} \\ &= \frac{-4\Gamma(\nu+1)\sin(\nu\pi/2)}{2^{\nu+2}\pi^{\nu+1}}\frac{P_0}{f_0^\nu}R^{-(\nu+1)}. \end{aligned} \quad (42)$$

(43)

[3] the effective height h of the wet troposphere is about one half of the nominal wet wet tropospheric scale height (Treuhaft and Lanyi 1987).

From the recurrence relation, see, e.g., (Arfken 1985, Eq. 5.217) or (Monin and Yaglom 1975, p. 90)

$$\Gamma(\nu)\Gamma(-\nu) = -\frac{\pi}{\nu \sin \pi\nu} \tag{44}$$

we derive

$$\Gamma(\nu)\Gamma(1-\nu) = \frac{\pi}{\sin \pi\nu} \tag{45}$$

$$\frac{\Gamma(1+\nu)\sin \pi\nu}{\pi} = \frac{\nu}{\Gamma(1-\nu)} \tag{46}$$

and using $\sin(2a) = 2 \sin a \cos a$ we find

$$\frac{\Gamma(1+\nu)\sin(\nu\pi/2)}{\pi} = \frac{\nu}{2\cos(\nu\pi/2)\Gamma(1-\nu)}. \tag{47}$$

Including (47) in (42) yield

$$< \phi_R^2 >= \frac{-2^2\nu}{2^{\nu+2}\pi^\nu 2\cos(\nu\pi/2)\Gamma(1-\nu)} \frac{P_0}{f_0^\nu} R^{-(\nu+1)}. \tag{48}$$

Using $\Gamma(p+1) = p\Gamma(p)$ and by rearranging terms we finally find

$$< \phi_R^2 > = \frac{-1}{2^{\nu+1}\pi^\nu \Gamma(-\nu)\cos(\nu\pi/2)} \frac{P_0}{f_0^\nu} R^{-(\nu+1)} \tag{49}$$

$$= C_\nu \frac{P_0}{f_0^\nu} R^{-(\nu+1)}, \tag{50}$$

or

$$D_\varphi(R) = C_\nu \frac{P_0}{f_0^\nu} R^{-(\nu+1)}, \tag{51}$$

as in equation (5). **End of the derivation.**

11 CONCLUSIONS

In this paper, we discussed some considerations which are essential for the construction of the variance-covariance matrix to include atmospheric signal in radar interferograms. We plan to improve the theory behind this, and produce a reliable stochastical model. Our final goal is the inclusion of all parameters into this model, and develop algorithms for the very large matrices which are the result of stacks of interferograms.

References

Agnew, D. C. (1992). The time-domain behaviour of power-law noises. *Geophysical Research Letters 19*(4), 333–336.

Arfken, G. (1985). *Mathematical Methods for Physicists* (3 ed.). Boston: Academic Press.

Bracewell, R. N. (1986). *The Fourier transform and its applications* (3 ed.). New York: McGraw-Hill.

Gradshteyn, I. S., I. M. Ryzhik, and A. Jeffrey (1994). *Table of integrals, series, and products* (5 ed.). Boston: Academic Press. Original Title: Tablitsy integralov, summ, ryadov i proizvediniy, 1965.

Hanssen, R. (1998). *Atmospheric heterogeneities in ERS tandem SAR interferometry*. DEOS Report no 98.1. Delft, the Netherlands: Delft University Press.

Ishimaru, A. (1978). *Wave Propagation and Scattering in Random Media*, Volume 2. New York: Academic Press.

Just, D. and R. Bamler (1994). Phase statistics of interferograms with applications to synthetic aperture radar. *Applied Optics 33*(20), 4361–4368.

Kolmogorov, A. N. (1941). Dissipation of energy in locally isotropic turbulence. *Doklady Akad. Nauk SSSR 32*(16). German translation in "Sammelban zur Statistischen Theorie der Turbulenz, Akademie Verlag, Berlin, 1958, p77.

Mandelbrot, B. B. and J. W. V. Ness (1968, October). Fractional Brownian motions, fractional noises and applications. *SIAM Review 10*(4), 422–438.

Monin, A. S. and A. M. Yaglom (1975). *Statistical Fluid Mechanics: Mechanics of Turbulence*, Volume 2. Cambridge: MIT Press. Original title: Statisich-eskaya gidromekhanika – Mekhanika Turbulenosti.

Newland, D. E. (1993). *Random vibrations, spectral and wavelet analysis* (3 ed.). Harlow: Longman.

Obukov, A. M. (1941). On the distribution of energy in the spectrum of turbulent flow. *Doklady Akad. Nauk SSSR 32*(19).

Ruf, C. S. and S. E. Beus (1997, March). Retrieval of tropospheric water vapor scale height from horizontal turbulence structure. *IEEE Trans. on Geoscience and Remote Sensing 35*(2), 203–211.

Tatarski, V. I. (1961). *Wave propagation in a turbulent medium*. New York: McGraw-Hill.

Treuhaft, R. N. and G. E. Lanyi (1987, March). The effect of the dynamic wet troposphere on radio interferometric measurements. *Radio Science 22*(2), 251–265.

i	a_i	i	a_i
0	−0.22318e+00	6	−0.47644e−02
1	0.10108e+01	7	0.43030e−03
2	−0.22470e+00	8	0.40255e−03
3	0.25715e−01	9	−0.16176e−04
4	0.32032e−01	10	−0.13693e−04
5	−0.44802e−02		

Table 1: Parameters for spatial structure function, (Treuhaft and Lanyi, 1987)

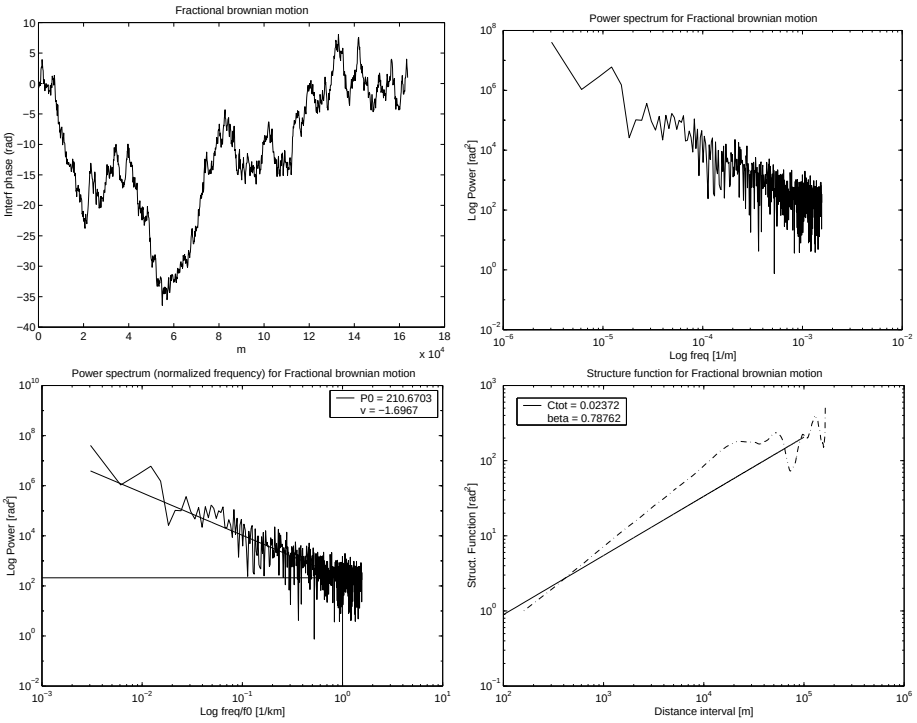

Figure 1: Fractional Brownian motion (a) Simulated fBm. (b) Power spectrum of fBm. (c) the same Power spectrum with f_0 chosen as 1 km. P_0 follows from this choice. We find that for fBm, $\nu \approx -5/3$ (d) The structure function related to the simulated signal. The solid line is the derived from the power spectrum using eq. (51), with $-(\nu+1) \approx 2/3$. The striped line is calculated directly from the data. Note that for large intervals, the estimation is not well determined.

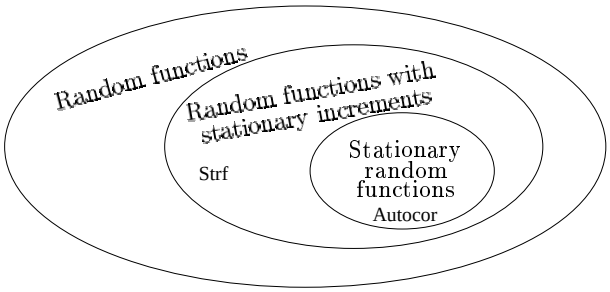

Figure 2: Schematic visualization of the three sets: random functions, random functions with stationary increments, and stationary functions. The covariance function is defined only for stationary functions, whereas the structure function is defined for both stationary functions and functions with stationary increments.

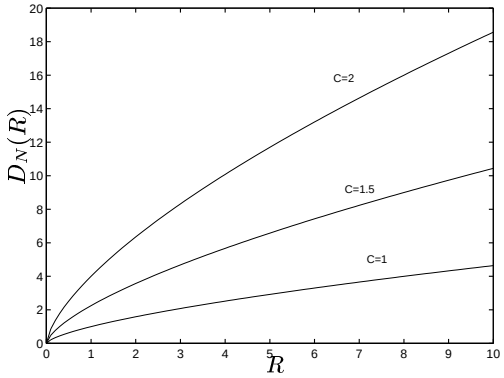

Figure 3: Example of the structure function $D_N(R) = C^2 R^{2/3}$, for $C = 1$, 1.5, and 2, using arbitrary units of length.

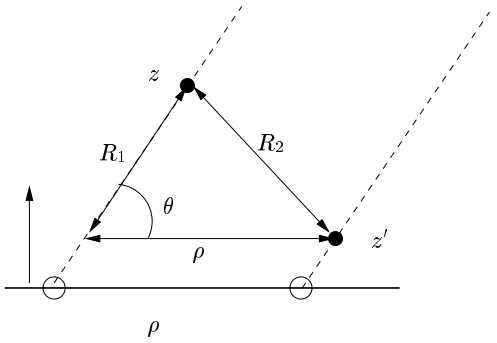

Figure 4: Geometric configuration for the integration along two paths, z and z', expressed in equation (24). In this sketch azimuth angle $\phi = 0$ is used.

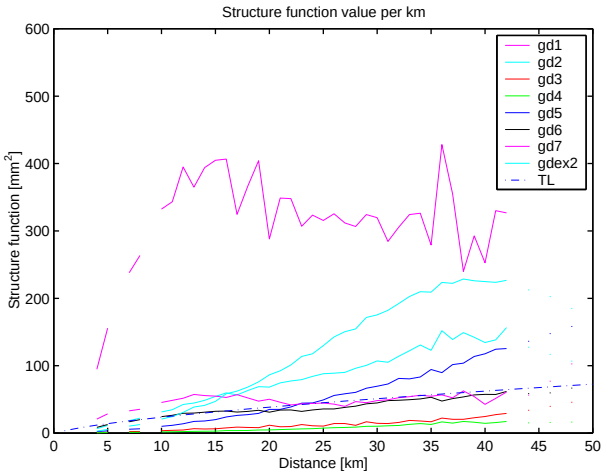

Figure 5: Derived structure functions for 8 interferogram segments of 50×50 km over Groningen, the Netherlands. For comparison we show the Treuhaft/Lanyi model as the striped line.

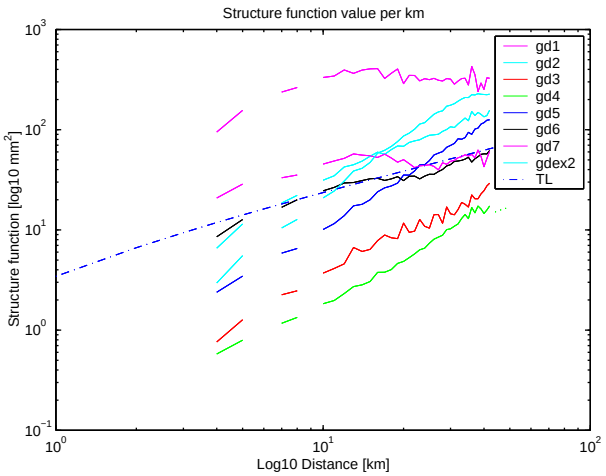

Figure 6: Derived structure functions for 8 interferogram segments of 50×50 km over Groningen, the Netherlands, using a log-log scale. For comparison we show the Treuhaft/Lanyi model as the striped line.

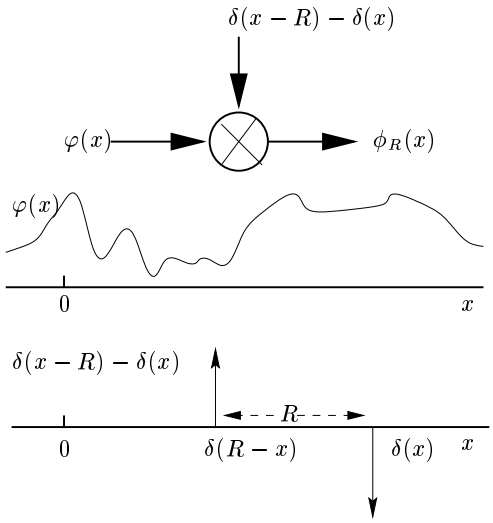

Figure 7: Dirac impulse convolution

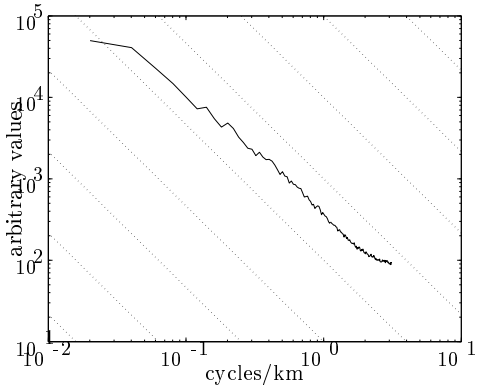

Figure 8: Rotational average spectrum of interferogram 1

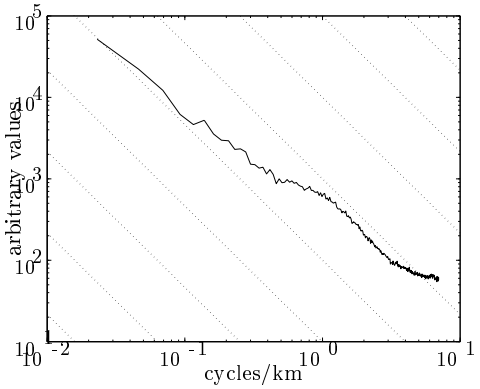

Figure 9: Rotational average spectrum of interferogram 2

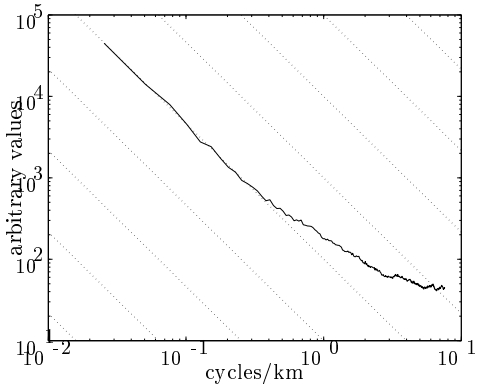

Figure 10: Rotational average spectrum of interferogram 3

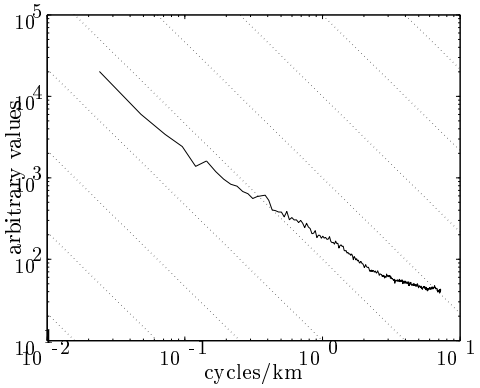

Figure 11: Rotational average spectrum of interferogram 4